

Warming advances top-down control and reduces producer biomass in a freshwater plankton community

MANDY VELTHUIS,^{1,†} LISETTE N. DE SENERPONT DOMIS,^{1,2} THIJS FRENKEN,¹ SUSANNE STEPHAN,^{1,3}
GARABET KAZANJIAN,⁴ RALF ABEN,^{1,5} SABINE HILT,⁴ SARIAN KOSTEN,^{1,5}
ELLEN VAN DONK,^{1,6} AND DEDMER B. VAN DE WAAL¹

¹*Department of Aquatic Ecology, Netherlands Institute of Ecology (NIOO-KNAW), Droevendaalsesteeg 10,
6708 PB Wageningen, The Netherlands*

²*Department of Aquatic Ecology and Water Quality Management, Wageningen University, P.O. Box 47,
6708 PB Wageningen, The Netherlands*

³*Department of Experimental Limnology, Leibniz-Institute of Freshwater Ecology and Inland Fisheries,
Alte Fischerhütte 2, 16775 Stechlin, Germany*

⁴*Department of Ecosystem Research, Leibniz-Institute of Freshwater Ecology and Inland Fisheries,
Müggelseedamm 301, 12587 Berlin, Germany*

⁵*Department of Aquatic Ecology and Environmental Biology, Institute for Water and Wetland Research,
Radboud University Nijmegen, P.O. Box 9010, 6500 GL Nijmegen, The Netherlands*

⁶*Department of Ecology and Biodiversity, University of Utrecht, P.O. Box 80.056, 3508 TB Utrecht, The Netherlands*

Citation: Velthuis, M., L. N. de Senerpont Domis, T. Frenken, S. Stephan, G. Kazanjian, R. Aben, S. Hilt, S. Kosten, E. van Donk, and D. B. Van de Waal. 2017. Warming advances top-down control and reduces producer biomass in a freshwater plankton community. *Ecosphere* 8(1):e01651. 10.1002/ecs2.1651

Abstract. Global warming has been shown to affect ecosystems worldwide. Warming may, for instance, disrupt plant herbivore synchrony and bird phenology in terrestrial systems, reduce primary production in oceans, and promote toxic cyanobacterial blooms in freshwater lakes. Responses of communities will not only depend on direct species-specific temperature effects, but also on indirect effects related to bottom-up and top-down processes. Here, we investigated the impact of warming on freshwater phytoplankton community dynamics, and assessed the relative contribution of nutrient availability, fungal parasitism, and grazing therein. For this purpose, we performed an indoor mesocosm experiment following seasonal temperature dynamics of temperate lakes and a warmed (+4°C) scenario from early spring to late summer. We assessed phytoplankton biomass, C:N:P stoichiometry and community composition, dissolved nutrient availabilities, fungal parasite (i.e., chytrid) prevalence, and zooplankton abundance. Warming led to an overall reduction in phytoplankton biomass as well as lower C:P and N:P ratios, while phytoplankton community composition remained largely unaltered. Warming resulted in an earlier termination of the diatom spring bloom, and an epidemic of its fungal parasite ended earlier as well. Furthermore, warming advanced zooplankton phenology, leading to an earlier top-down control on phytoplankton in the period after the spring bloom. Linear model analysis showed that most of the observed variance in phytoplankton biomass was related to seasonal temperature dynamics in combination with zooplankton abundance. Our findings showed that warming advanced grazer phenology and reduced phytoplankton biomass, thereby demonstrating how bottom-up and top-down related processes may shape future phytoplankton dynamics.

Key words: chytrid dynamics; global warming; phytoplankton community dynamics; seasonal succession; zooplankton phenology.

Received 5 July 2016; revised 18 November 2016; accepted 21 November 2016. Corresponding Editor: Ryan Allen Sponseller.

Copyright: © 2017 Velthuis et al. This is an open access article under the terms of the Creative Commons Attribution License, which permits use, distribution and reproduction in any medium, provided the original work is properly cited.

† **E-mail:** m.velthuis@nioo.knaw.nl

INTRODUCTION

Currently, our climate is changing at an unprecedented rate. Global temperatures have been rising for decades and are predicted to rise further with an additional 3–5°C over the next century (IPCC 2014). This global warming has been shown to affect a wide range of ecosystems. For example, warming may disrupt plant herbivore synchrony and bird phenology in terrestrial systems (Both et al. 2009), reduce primary production in oceans (Polovina et al. 2008), and promote the occurrence of toxic cyanobacterial blooms in freshwater lakes (Paerl and Huisman 2008, Kosten et al. 2012). Predicting ecosystem responses to warming, however, still remains a major challenge, and current observations are not unambiguous (Donnelly et al. 2011). For instance, warming can cause both an increase (Yvon-Durocher et al. 2011, Shurin et al. 2012) or a decrease (Winder and Schindler 2004a) in top-down control on freshwater phytoplankton communities.

Warming may also directly affect phytoplankton growth, though the response will depend on specific growth optima. For instance, some species with lower growth optima responded negatively to warming (Butterwick et al. 2005), while others responded positively (van Donk and Kilham 1990). Consequently, responses of phytoplankton may depend on the community composition. Indeed, a variety of effects have been reported for different communities, ranging from an advanced timing (Hansson et al. 2013) and increased community growth rate and carrying capacity (De Senerpont Domis et al. 2014) of chlorophyte-dominated communities to shifts in community composition favoring cyanobacteria (O'Neil et al. 2012) or phytoflagellates (Strecker et al. 2004). Warming may also indirectly affect phytoplankton by changes in nutrient availability. Specifically, warming may lead to an increase in nutrient concentrations by elevated phosphorus loading from the catchment (Jeppesen et al. 2009), enhanced mineralization rates (Gudasz et al. 2010), and increased evaporation (De Senerpont Domis et al. 2013), promoting phytoplankton growth. On the other hand, warming may enhance thermal stratification of the water column and thereby reduce nutrient input from deeper waters into the upper mixed layer (Polovina et al. 2008, Lewandowska et al. 2014), which can impede phytoplankton

growth. Warming in concert with changes in nutrient availability may alter the elemental composition of phytoplankton (Rhee and Gotham 1981, De Senerpont Domis et al. 2014) and thereby affect their nutritional quality for higher trophic levels (Sterner and Elser 2002, Biermann et al. 2015). For instance, lowered nutritional quality of phytoplankton resulted in reduced growth rates of daphnids (Urabe et al. 2003) and rotifers (Jensen and Verschoor 2004).

Warming has also been shown to directly affect zooplankton growth and reproduction. For example, warming may enhance somatic growth rates of *Daphnia* (McFeeters and Frost 2011), reproduction rates of rotifers (Kauler and Enesco 2011), and zooplankton hatching rates (Weydmann et al. 2015). Consequently, warming can lead to higher zooplankton biomass (Kratina et al. 2012) and advance the timing of peak zooplankton abundance (Adrian et al. 2006, Hansson et al. 2013). Besides zooplankton, fungal parasites (i.e., chytrids) can play a major role in shaping plankton communities (van Donk and Ringelberg 1983), particularly because they can be highly host specific (Ibelings et al. 2004). Moreover, their epidemics may depend on temperature. For instance, in years with relatively warm winters, chytrid prevalence did not reach epidemic levels, but did prevent the formation of a phytoplankton spring bloom (Ibelings et al. 2011). In contrast, warming may also lead to lowered zoospore production (Bruning 1991), possibly reducing the encounter rate of phytoplankton with the zoospores. Such temperature-driven changes in zooplankton and parasite dynamics can, in turn, feed back on phytoplankton biomass build-up and community composition.

Due to this complex interplay between indirect and direct effects, predicting the impact of warming on plankton communities is not straightforward. Incorporation of multiple trophic levels in experimental warming studies is needed to better comprehend the effects of temperature on plankton communities. Here, we studied the effects of warming on a temperate freshwater plankton community in ~1000-L indoor mesocosms, over a period from spring to summer. The mesocosms were exposed to a temperature scenario representing ambient Dutch conditions (control), as well as a +4°C scenario (warm treatment). We followed changes in phytoplankton biomass, community composition, and elemental composition,

as well as dissolved nutrient availability, zooplankton dynamics, and the prevalence of fungal parasites over time.

METHODS

Experimental set-up

Experiments were performed in eight 988 L indoor mesocosms referred to as limnotrons (1.37 m depth, 0.97 m diameter, see also Verschoor et al. 2003) filled with 908 L of tap water and 80 L of pre-sieved sediment (5 mm mesh size). Sediment was collected on 13-02-2014 from a mesotrophic shallow pond in Wageningen, The Netherlands (51°59'16.3" N 5°40'06.0" E), with an additional small portion (<10% volume) from a nearby eutrophic pond (51°58'56.7" N 5°43'34.5" E) to allow for a more diverse initial benthic community. Prior to phytoplankton inoculation and nutrient addition, water was circulated between all limnotrons for 2 days to ensure equal starting conditions. For the phytoplankton inoculum, 300 L of water from the first pond was concentrated over a 30- μ m plankton net, and distributed equally over all limnotrons. Similarly, a small portion (<15% inoculum volume) was sampled from the second pond.

Surface mixing was achieved by an aquarium pump (EHEIM compact 300; EHEIM GmbH & Co. KG, Deizisau, Germany), positioned just below the water surface. Surface gas diffusion was promoted by two compact axial fans (AC axial compact fan 4850 Z; EBM-papst St. Georgen GmbH & Co. KG, Georgen, Germany) with an air flow of 100 m³/h. The incident light intensity was constant throughout the experiment with 175 ± 25 (mean \pm SD) μ mol photons·m⁻²·s⁻¹, provided by two HPS/MH lamps (CDM-TP Elite MW 315–400 W; AGRILIGHT B.V., Monster, The Netherlands). The light/dark cycle followed typical Dutch seasonality (Appendix S1: Fig. S1). Nutrients were added to final concentrations of 86 ± 19 , 2.4 ± 0.8 , and 152 ± 37 μ mol/L (mean \pm SD) of NO₃⁻, PO₄³⁻, and Si, respectively, after which the experiment started on 06-03-2014. Temperature treatments ($n = 4$) included an average seasonal water temperature cycle based on Dutch conditions (control), and the same seasonal temperature cycle +4°C (warm). To obtain these treatments, temperature was logged every minute and limnotrons were automatically cooled or

heated by a computer-controlled (SpecView 32/859; SpecView Ltd., Uckfield, UK) custom-made climate control system. From 03-08 until 10-08, a heatwave of an additional +4°C was simulated in both treatments (Appendix S1: Fig. S1). Here, we report the results from the start of the experiment until 15-08.

Twice a week, depth-integrated water samples of 3.5 L for phytoplankton community composition, seston elemental composition, chlorophyll-*a* concentrations, chytrid prevalence of infection, and dissolved nutrients were taken from the center of the limnotron with a transparent sampling tube of 1 m length. Water samples were subsequently fractionated into three size classes (unfiltered, <220 μ m, and <85 μ m) that were used for distinct analyses as described below. Once a week, zooplankton community composition, inorganic carbon concentrations, light availability, and abundance of floating and filamentous algae (when present) were also analyzed. Biomass of wall periphyton (hereafter termed periphyton) and benthic algae were analyzed on a biweekly basis. Methods for light availability and periphyton, as well as benthic, floating, and filamentous algae, are described in Appendices S3 and S4, respectively. To account for water losses via evaporation and sampling, mesocosms were topped up with demineralized water twice a week. From June onward, minor nutrient losses by sampling were compensated by weekly additions of 308 μ mol NO₃⁻ and 12 μ mol PO₄³⁻, representing 0.4% and 0.5% of initial concentrations, respectively.

Phytoplankton community composition

Unfiltered water samples (5 mL) were fixed with alkaline Lugol's iodine solution and stored in the dark. Microscopic determination of phytoplankton to genus level was performed in 2.2 mL subsamples on an inverted microscope (DMI 4000B; Leica Microsystems CMS GmbH, Mannheim, Germany), counting up to 200 individuals or 100 fields of view using Utermöhl counting chambers with a settling time of at least one hour.

For flow cytometric analysis (MoFlo Legacy Cell Sorter; Beckman Coulter, Miami, Florida, USA), 4 mL samples from the <85- μ m fraction were fixed with a paraformaldehyde–glutaraldehyde solution (6.75/1) to a final concentration of 1% (v/v) and stored at 5°C for a maximum period of 6 weeks prior to analysis. Calibration with 2- and 30- μ m

beads allowed further fractionation of the phytoplankton in size classes <2, 2–30, and 30–85 µm, based on the particle time of flight and side scatter.

Seston elemental composition

For analysis of particulate organic carbon (C), nitrogen (N), and phosphorus (P), samples from the <220-µm fraction were taken once a week, filtered on pre-washed GF/F filters (Whatman, Maidstone, UK), dried at 60°C overnight, and stored dry and dark. Using a hole puncher, 6 × 3 mm subsamples were taken from the GF/F filters (~13%). These subsamples were thereafter folded together into a tin cup (Elemental Microanalysis, Okehampton, UK) and analyzed for particulate C and N on a FLASH 2000 NC elemental analyzer (Brechtbuhler Incorporated, Interscience B.V., Breda, The Netherlands). The remainder of the filter was combusted in a Pyrex glass tube at 550°C for 30 min. Subsequently, 5 mL of persulfate (2.5%) was added and samples were autoclaved for 30 min at 121°C. Digested P (as PO_4^{3-}) was measured on a QuAatro39 Auto-Analyzer (SEAL Analytical Ltd., Southampton, UK).

Chlorophyll-a concentrations

Chlorophyll-*a* concentrations were determined from the <220-µm fraction twice a week by means of chlorophyll-*a* fluorescence. Chlorophyll-*a* fluorescence was measured in triplicate on a Phyto-PAM with an Optical Unit ED-101US/MP (Heinz Walz GmbH, Effeltrich, Germany), using a 0.2 µm filtered water sample for background correction. These chlorophyll-*a* fluorescence measurements were calibrated with ethanol extractions at several time points during the experiment, for which 100 mL water samples of the <220-µm fraction were filtered on GF/F filters (Whatman) and stored at –20°C. Frozen GF/F filters were thawed and spectrophotometrically analyzed according to Lorenzen (1967), using an absorption coefficient for chlorophyll-*a* of 12.264 (Roijackers 1981). Linear regression of the ethanol extraction data and chlorophyll-*a* fluorescence ($R^2 = 0.60$; $n = 189$) yielded a conversion factor of 0.87 to calculate chlorophyll-*a* concentrations from the fluorescence signal.

Total inorganic carbon, nutrients, and light

Once a week, subsamples from the depth-integrated water sample were taken carefully (to

prevent gas exchange) for total inorganic carbon (TIC) analysis. The sample was stored in 3 mL non-evacuated exetainers (Labco, Lampeter, UK) at 4°C. Total inorganic carbon was measured on an AO2020 Continuous Gas Analyzer (ABB, Zürich, Switzerland) within 24 h. Temperature was determined as a daily average from the continuously logged temperature, and pH measurements (SenTix 41 pH electrode; WTW GmbH, Weilheim, Germany) were performed on the depth-integrated water sample. CO_2 concentrations were calculated from TIC, pH, and temperature according to Harrison (2007) using freshwater carbon dissociation constants (Dickson and Millero 1987).

Water samples for dissolved inorganic nutrients were taken from the <220-µm fraction twice a week, filtered over pre-washed GF/F filters (Whatman), and the filtrate was stored at –20°C. Concentrations of dissolved nutrients (PO_4^{3-} , NO_2^- , NO_3^- , and NH_4^+) of thawed samples were determined on a QuAatro39 Auto-Analyzer (SEAL Analytical Ltd.). For silicon (Si) measurements, thawed samples were acidified with nitric acid (69%) to yield a final concentration of 1% (v/v) and analyzed by inductively coupled plasma optical emission spectrometry (ICP-OES, Iris Intrepid II; Thermo Fisher Scientific, Waltham, Massachusetts, USA).

Chytrid prevalence and zooplankton community composition

Chytrid prevalence of infection was analyzed for the diatom species *Synedra* as described in Frenken et al. (2016). Biweekly samples were stained with 4% (v/v) Calcofluor White, and at least 200 *Synedra* cells or 20 fields of view were counted on an inverted epifluorescence microscope (DMI 4000B; Leica Microsystems CMS GmbH). The number of infected (*i*) or uninfected (*u*) cells was assessed, and the prevalence of infection could subsequently be calculated as $P = i/(i + u)$, modified after Rasconi et al. (2009) and Gsell et al. (2013).

Depth-integrated samples for assessing zooplankton community composition were taken weekly, and every second day during the heat wave. In total, 14 L of water was sampled (7 L at the middle of the limnotron and 7 L at the vicinity of the wall), concentrated on a 75-µm mesh, fixed with 96% ethanol, and stored at room temperature.

Zooplankton specimens were counted using a stereomicroscope (Leica WILD MZ8; Leica Microsystems, Wetzlar, Germany). At least 100 specimens of the most abundant taxa were counted. Rotifers and cladocerans were determined to genus level (Pontin 1978, Witty 2004), whereas copepods were distinguished by order. Copepod nauplii were counted, but not distinguished taxonomically.

Statistical analyses

All statistical analyses were carried out in R (R Core Team 2015). Time series of phytoplankton dynamics, bottom-up and top-down control were tested with linear mixed-effect (LME) models (function *lme* with the maximum-likelihood method from package *nlme*; Pinheiro et al. 2015), integrating time nested within limnotron identity as random effects. *P*-values were obtained by pairwise comparison of the treatment \times time model (to account for interaction effects between temperature treatment and time), treatment + time model (treatment model with added fixed factor time), and treatment and time model separately (function *anova*). Data were tested for normality and homogeneity of variance (*shapiro.test* and *var.test*, respectively) and were log- or square-root-transformed when necessary.

Changes in phenology in response to warming were determined based on identification of the cardinal dates (i.e., time of start, peak, and end) of bloom dynamics using Weibull fits from the *cardinal* package (Rolinski et al. 2007). Cardinal dates for chlorophyll-*a* during the spring bloom, chytrid prevalence of infection, and abundance of rotifers, cladocera, and copepods were determined for each limnotron (function *fitweibull6*). For the chlorophyll-*a* spring bloom, data from 06-03 to 29-05 were used. Overall abundance was calculated as the area under the respective Weibull fit curve. Treatment effects on these cardinal dates and overall abundance were tested with Student's *t*-test (function *t.test*).

General linear models were used to explore the relationship of chlorophyll-*a* concentration with abiotic factors (dissolved inorganic nitrogen (DIN), dissolved inorganic phosphorus (DIP), dissolved Si, and logged temperature) and biotic factors (zooplankton abundance and chytrid prevalence of infection). Missing values were interpolated with the *na.spline* function from the *zoo* package

(Zeileis and Grothendieck 2005). Variable selection per limnotron was based on Akaike information criterion (function *stepAIC* from MASS package; Venables and Ripley 2002), and the variables that were selected in at least one of the limnotrons were used in further analysis. We ran linear models separately for each limnotron in order to assess the contribution of each variable to chlorophyll-*a* dynamics, as well as the variation of this contribution between limnotrons. To check for the presence of temporal autocorrelation, the residuals from the model fits were tested with the function *auto.arima* (package *forecast* from Hyndman 2015) and ARIMA transformed when necessary. Relative contribution for each of the independent variables to the R^2 of the models was determined with the *calc.relimp.lm* function with *lmg* metrics from the *relaimpo* package (Grömping 2006). Relative contribution per variable was then tested within model fits and between treatments with a two-way ANOVA (function *aov*).

RESULTS

Phytoplankton dynamics

Chlorophyll-*a* concentrations increased during the first 18 days of the experiment to maximum values of 31 ± 13 and 27 ± 6 $\mu\text{g/L}$ (mean \pm SD) for the control and warm treatment, respectively (Fig. 1). An additional increase in chlorophyll-*a* was observed in the control treatment from 02-06 until 30-06, as well as during the heatwave. Chlorophyll-*a* concentrations were generally lower in the warm treatment over the entire experimental period (LME; $P < 0.001$; Table 1, Fig. 1), and this difference was about 20% during the spring bloom (Weibull; $P < 0.05$; Table 2). The spring bloom consisted mostly of large cells (i.e., >30 μm , Fig. 2), dominated by the pennate diatom *Synedra* (Appendix S2: Fig. S2). After the spring bloom, the phytoplankton community shifted to pico- and nanophytoplankton (i.e., size classes 0–2 and 2–30 μm , respectively) from 24-04 until 13-07 (Fig. 2). The second phytoplankton bloom in the control treatment mainly consisted of the mixotrophic chrysophyte *Dinobryon*, the cyanobacterium *Pseudanabaena*, and small unicellular chlorophytes (Appendix S2: Fig. S2). Thereafter, from 13-07 until the end of the experiment, the phytoplankton community was mostly comprised of nanophytoplankton (i.e., size class 2–30 μm , Fig. 2),

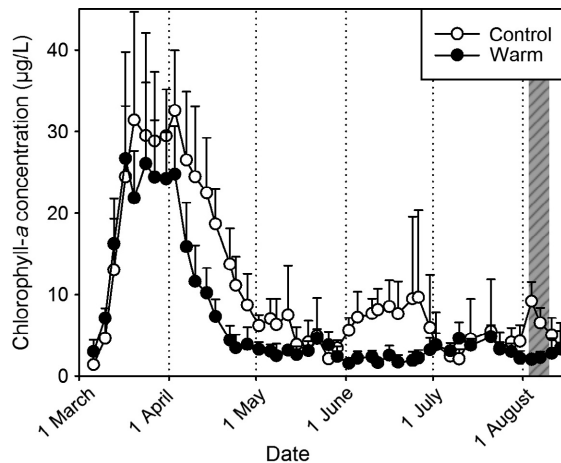


Fig. 1. Phytoplankton biomass, expressed as chlorophyll-*a* concentration, in control (open circles) and warm (closed circles) treatments. Values denote mean \pm SD ($n = 4$). Period of heatwave is indicated by the gray bar.

dominated by the cyanobacterium *Chroococcus* and small chlorophytes (Appendix S2: Fig. S2). No shifts in cell size distribution of the phytoplankton community in response to warming

were observed, as all three size classes showed largely comparable dynamics in both treatments (Fig. 2). All size classes showed significantly lower densities in the warm treatment (LME; $P < 0.05$; Table 1, Fig. 2).

Seston elemental composition

Seston C:N, C:P, and N:P ratios increased during the phytoplankton spring bloom, reaching maximum values of 13.3 ± 0.6 , 510 ± 33 , and 39.3 ± 4.8 , respectively, in the control and 13.4 ± 1.3 , 436 ± 82 , and 32.8 ± 6.9 (mean \pm SD) in the warm treatment (Fig. 3). After the spring bloom, C:N ratios decreased and showed dynamic changes in the vicinity of the Redfield ratio. In June, C:P and N:P ratios decreased toward the Redfield ratio in the warm treatment. In the control treatment, the C:P ratio remained higher, while N:P ratios increased to a maximum value of 23 ± 2.0 (mean \pm SD) on 19-6. During the heatwave, C:P and N:P ratios showed a rapid decline in both the control and warm treatment, while C:N ratios only dropped in the warm treatment. Seston C:N, C:P, and N:P ratios were generally lower in the warm treatment (LME; $P < 0.05$; Table 1, Fig. 3).

Table 1. Summary of linear mixed-effect (LME) models, describing the effect of warming, time, and their interaction on phytoplankton community characteristics (biomass and stoichiometry), bottom-up control (i.e., nutrient concentrations), top-down control (chytrid prevalence and zooplankton numbers), and competing algae (periphyton, benthic, filamentous, and floating algae).

Factor	Variable	Unit	L-ratio		
			Treatment	Time	Treatment \times Time
Phytoplankton	Chlorophyll- <i>a</i>	$\mu\text{g/L}$	13.0***	421.4***	170.3***
	Phytoplankton 0–2 μm	cells/mL	4.4*	496.2***	114.4**
	Phytoplankton 2–30 μm	cells/mL	4.9*	602.7***	118.4***
	Phytoplankton 30–85 μm	cells/mL	11.0***	752.1***	98.2**
	C:N	molar	4.0*	273.6***	16.1
	C:P	molar	8.6**	202.7***	59.0***
	N:P	molar	5.8*	145.0***	62.3***
Bottom-up	DIN	$\mu\text{mol/L}$	0.3	802.2***	87.1***
	DIP	$\mu\text{mol/L}$	0.0	809.8***	47.7
	Si	$\mu\text{mol/L}$	0.3	282.4***	26.7*
Top-down	Rotifer abundance	individuals/L	9.7**	194.7***	121.3***
	Cladoceran abundance	individuals/L	5.1*	180.4***	126.0***
	Copepod abundance	individuals/L	0.5	196.5***	99.6***
	Chytrid prevalence	%	4.4*	154.2***	93.0***
Competing algae	Periphyton	$\mu\text{g chlorophyll-}a/\text{cm}^2$	0.2	263.3***	6.6
	Benthic algae	$\mu\text{g chlorophyll-}a/\text{cm}^2$	0.8	45.8***	9.2
	Filamentous algae	PVI	4.1*	3.7	12.1
	Floating algae	% cover	5.9*	12.3	13.6*

Notes: PVI, percent volume infested; DIN, dissolved inorganic nitrogen; DIP, dissolved inorganic phosphorus. Significant outcomes are indicated in boldface, with $P < 0.05$ (*), $P < 0.01$ (**), and $P < 0.001$ (***).

Table 2. Summary of the Weibull fits, showing *P*-values for the difference between treatments of time-integrated abundance (i.e., area under fit) and timing of the dynamics (i.e., cardinal dates for start, mid, and end of the peak).

Variable	Total abundance	Cardinal dates		
	Area under fit	Start	Mid	End
Chlorophyll- <i>a</i> (spring bloom)	0.03 (–19.7)	0.09	0.12	0.64
Chytrid prevalence	0.07	0.50	0.24	0.02 (–17.6)
Rotifers	0.85	0.39	0.07	0.03 (–37.0)
Cladocera	0.17	0.02 (–19.0)	0.01 (–23.1)	0.13
Copepods	0.92	0.14	0.04 (–48.6)	0.29

Notes: The treatment effect is given between parentheses and indicates the relative deviation from control as % for total abundance and as number of days for the cardinal dates. Significant differences are indicated in boldface.

Abiotic conditions

Dissolved inorganic nitrogen (DIN) was depleted within 21 and 28 days after the start of the experiment in the warm and control treatments, respectively (Fig. 4a). DIN increased to near initial concentrations from 02-06 and 19-06 onward in the warm and control treatments, respectively. During this period, $\text{NO}_3^- : \text{NH}_4^+$ ratios were higher in the warm treatment (LME; *L*-ratio = 6.2; $P < 0.05$; Appendix S3: Fig. S3a). Dissolved inorganic phosphorus (DIP) was rapidly depleted within 11 days in both treatments, while dissolved Si was depleted after 28 and 35 days in the warm and control treatments, respectively (Fig. 4b, c). Both DIP and Si remained low for the remainder of the experiment. During the spring bloom, CO_2 concentrations decreased to 5.2 ± 1.4 and 6.3 ± 1.2 $\mu\text{mol/L}$ (mean \pm SD) in the control and warm treatments, respectively (Appendix S3: Fig. S3b). After the spring bloom, CO_2 concentrations slowly increased to supersaturating levels of up to 135 $\mu\text{mol/L}$ (i.e., a pCO_2 of ~ 1400 μatm). Dissolved CO_2 concentrations were generally higher in the warm treatment (LME; *L*-ratio = 6.7; $P < 0.01$; Appendix S3: Fig. S3b), while no treatment effect was observed on the concentrations of DIN, DIP, and dissolved Si (Table 1, Fig. 4).

Periphyton and benthic, filamentous, and floating algae

Biomass of periphyton gradually increased in both treatments after the spring bloom until reaching maximum values of 1.2 ± 0.96 μg chlorophyll-*a*/ cm^2 at 04-08 in the control and 1.5 ± 0.67 μg chlorophyll-*a*/ cm^2 (mean \pm SD) at 02-06 in the warm treatment (Appendix S4: Fig. S4a). Simultaneously, biomass of benthic

algae increased to maximum values on 16-06 of 0.78 ± 0.78 and 0.64 ± 0.77 μg chlorophyll-*a*/ cm^2 (mean \pm SD) in the control and warm treatments, respectively (Appendix S4: Fig. S4c). No difference in overall periphyton biomass, nor in biomass of benthic algae, was observed between treatments during the investigated period (Table 1). From 01-07 onward, abundance of filamentous and floating algae increased reaching maximum values of approximately 10% percent volume infested (PVI) and 20% cover, respectively (Appendix S4: Fig. S4b, d). As a result, average underwater light availability decreased over the experimental period (Appendix S3: Fig. S3c). In the warm treatment, PVI of filamentous algae was generally lower, while the cover percentage of floating algae was higher (LME; $P < 0.05$; Table 1). No difference in the underwater light availability was observed between the treatments (Appendix S3: Fig. S3c).

Chytrid and zooplankton dynamics

The *Synedra* spring bloom endured a chytrid infection with maximum prevalence of infection at 24-04 of $38\% \pm 21\%$ and $41\% \pm 20\%$ (mean \pm SD) in the control and warm treatments, respectively. The epidemic ended 18 days earlier in the warm treatment (Weibull; $P < 0.05$; Table 2, see also Frenken et al. 2016), and the dynamics in prevalence of infection differed between treatments (LME; $P < 0.05$; Table 1, Fig. 5a).

The zooplankton community consisted mainly of rotifers and cladocerans, while copepod abundance remained low throughout the experiment (Fig. 5). After the spring bloom, rotifer numbers increased to maximal 1092 ± 260 and 1738 ± 735 individuals/L in the control and warm treatments, respectively, and were dominated by

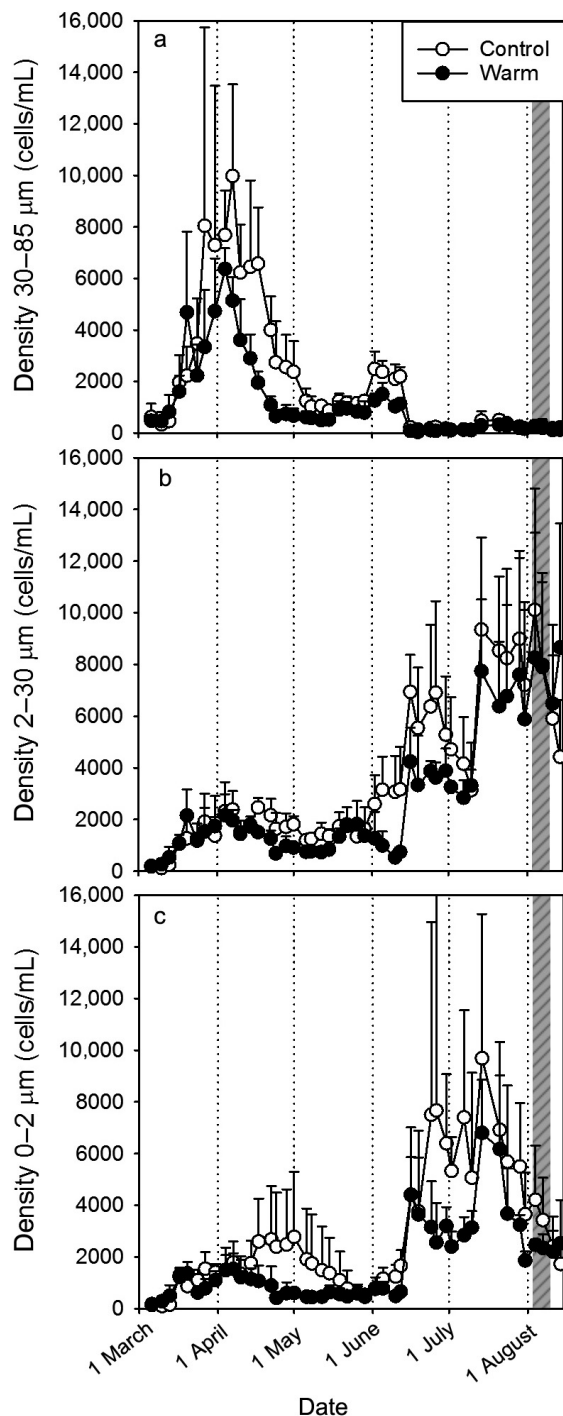


Fig. 2. Cell densities of phytoplankton size classes with (a) 30–85 μm , (b) 2–30 μm , and (c) 0–2 μm in control (open circles) and warm (closed circles) treatments. Values denote mean \pm SD ($n = 4$). Period of heatwave is indicated by the gray bar.

Keratella (Fig. 5b). Numbers of cladocera increased afterward, reaching maximum numbers of 1524 ± 1732 and 2176 ± 2145 individuals/L in the control and warm treatments, respectively, and were dominated by *Bosmina* (Fig. 5c). In the warm treatment, the end of the rotifer population peak advanced by 37 days, while the start of the

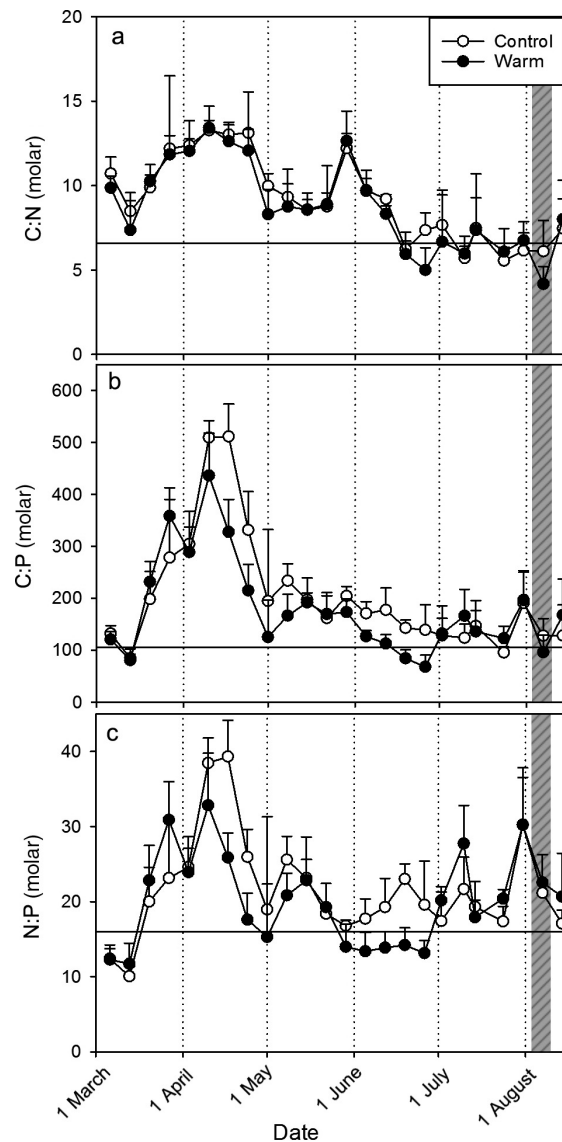


Fig. 3. Seston elemental composition with (a) C:N, (b) C:P, and (c) N:P molar ratios in control (open circles) and warm (closed circles) treatments. Values denote mean \pm SD ($n = 4$). Period of heatwave is indicated by the gray bar, and horizontal black lines depict the Redfield ratios.

cladoceran population peak advanced by 19 days (Weibull; $P < 0.05$; Table 2). The timing of peak biomass of cladocera and copepods advanced by 23 and 49 days, respectively (Weibull; $P < 0.05$; Table 2). Also, the timing of population peak biomass of rotifers seemed to advance, though changes were not significant (Weibull; $P = 0.07$;

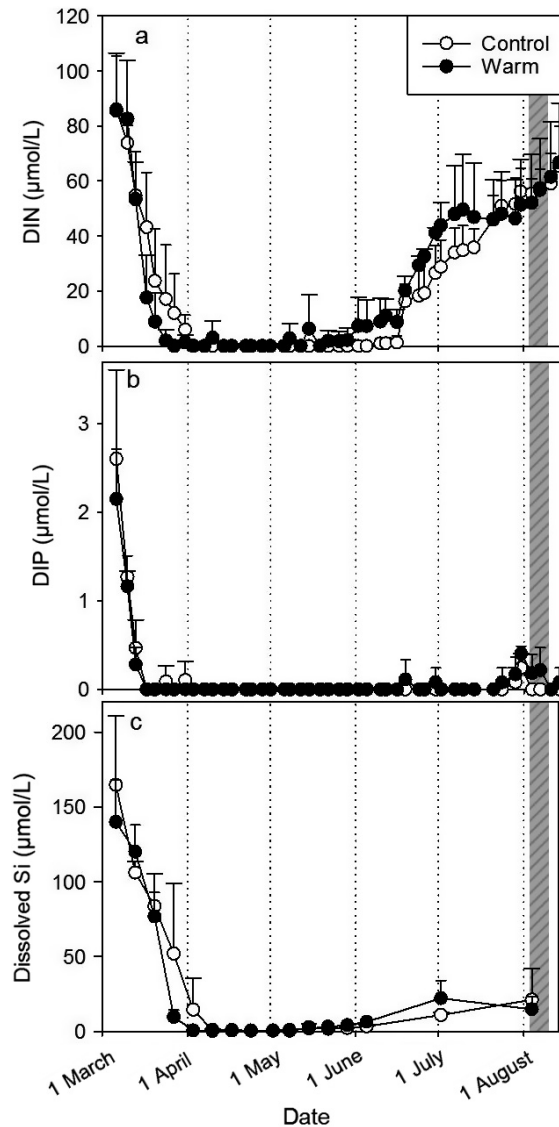


Fig. 4. Inorganic nutrient concentrations with (a) dissolved inorganic nitrogen (DIN), (b) dissolved inorganic phosphorus (DIP), and (c) dissolved Si in control (open circles) and warm (closed circles) treatments. Values denote mean \pm SD ($n = 4$). Period of heatwave is indicated by the gray bar.

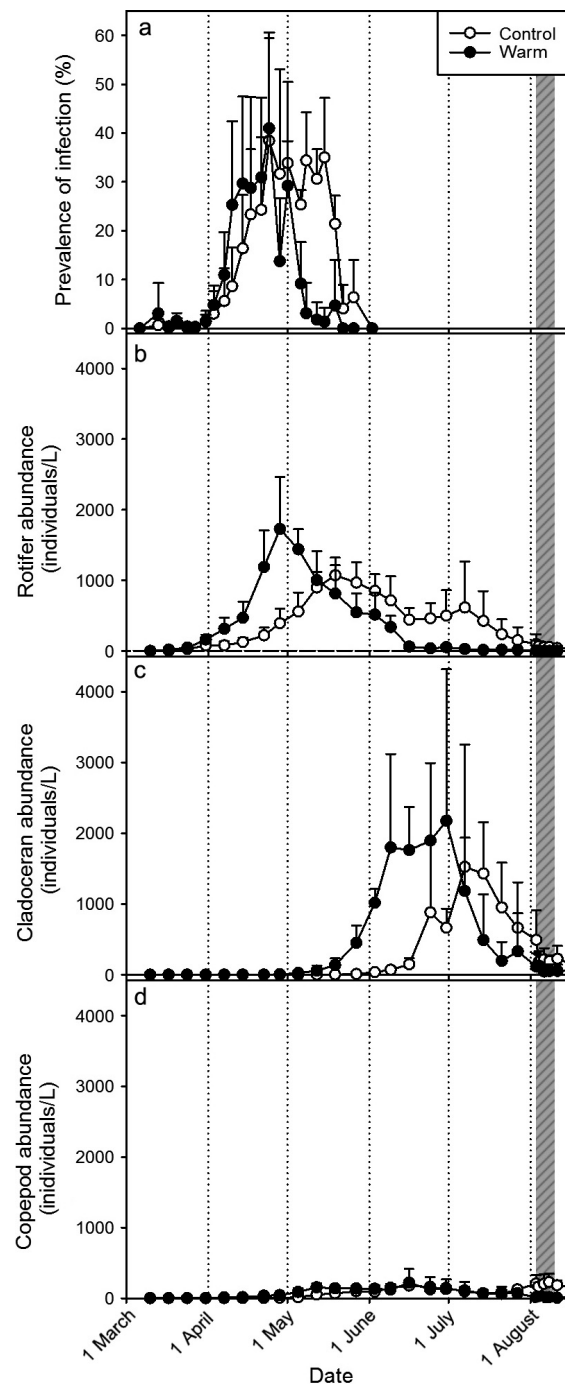


Fig. 5. Parasite and grazer dynamics with (a) chytrid prevalence, and (b) rotifer, (c) cladoceran, and (d) copepod abundance in control (open circles) and warm (closed circles) treatments. Values denote mean \pm SD ($n = 4$). Period of heatwave is indicated by the gray bar.

Table 3. Summary of results from the linear model of chlorophyll-*a* dynamics, indicating contribution of multiple variables to the total R^2 in control and warm treatments.

Factor	Variable	Contribution to R^2	
		Control	Warm
Total model		0.66 ± 0.20	0.72 ± 0.05
Seasonal temperature		0.24 ± 0.09	0.30 ± 0.07
Bottom-up	DIP	0.09 ± 0.04	0.09 ± 0.04
	DIN	0.10 ± 0.02	0.09 ± 0.02
	Si	0.05 ± 0.01	0.07 ± 0.03
Top-down	Zooplankton	0.18 ± 0.10	0.19 ± 0.09
	Chytrid prevalence	0.09 ± 0.04	0.05 ± 0.02

Note: Values denote mean ± SD ($n = 4$) of R^2 values.

Table 2). No treatment effect on total zooplankton abundance was observed (Table 2).

Variables explaining phytoplankton chlorophyll-*a* dynamics

The linear model explained 66% ± 20% and 72% ± 5% (mean ± SD) of the total variance in chlorophyll-*a* in the control and warm treatments, respectively (Table 3). This explained variance could be associated with different variables. The variables temperature and zooplankton contributed around 0.27 and 0.19, respectively, to the R^2 of the total model (Table 3). Contributions of the remaining variables (DIP, DIN, prevalence, and Si) were comparable and ranged between 0.10 and 0.05. No treatment effect was observed in the contribution of the different variables to the total variance in chlorophyll-*a* concentrations ($F_{1,36} = 0.25$; $P > 0.5$, Table 3).

DISCUSSION

Global warming is predicted to have profound effects on food-web structure and functioning, and phenological shifts in top-down control of primary producers have been reported in a diverse range of ecosystems (Donnelly et al. 2011). We performed an indoor mesocosm experiment to study the impacts of warming on a freshwater plankton food web. Although these mesocosm systems do not fully represent natural conditions, they are ideal for studying complex plankton interactions in a relatively controlled environment. Our results demonstrate that experimental warming reduced

planktonic primary producer biomass (Figs. 1, 2), while biomass of planktonic consumers generally remained unchanged (Table 2). This is in line with earlier studies in both marine and freshwater ecosystems (O'Connor et al. 2009, Berger et al. 2010, Yvon-Durocher et al. 2011, Kratina et al. 2012, Shurin et al. 2012, Sommer et al. 2012, Hansson et al. 2013). Warming furthermore advanced grazer phenology and the end of the parasite epidemic (Fig. 5, Table 2), thereby causing a temporal advancement in top-down control. Earlier studies have also shown advanced consumer phenology in response to warming in a variety of ecosystems, for instance for freshwater zooplankton (Adrian et al. 2006), marine turtles (Mazaris et al. 2008), and Mediterranean butterflies (Stefanescu et al. 2003). Such warming-induced shifts in top-down control may have profound consequences for producer community dynamics (Strecker et al. 2004, Winder and Schindler 2004a).

Phytoplankton community dynamics

The initial phytoplankton bloom was dominated by the large diatom *Synedra*, with a subsequent increase in smaller pico- and nanophytoplankton (Fig. 2). Spring blooms of large diatoms are observed in natural systems (van Donk and Ringelberg 1983, Sommer et al. 1986) and may reflect their ability to proliferate at lower temperatures provided that nutrients, including silicate, are available. The delayed development of smaller phytoplankton may not only be due to depleted nutrient conditions and/or high rotifer abundance at the end of the spring bloom, but may also be partially affected by the size fraction of the inoculum (i.e., >30- μm), which further favored the proliferation of larger phytoplankton.

During the spring bloom, seston elemental C:N, C:P, and N:P ratios increased and exceeded the Redfield ratio in both treatments (Fig. 3). This was associated with the depletion of both DIN and DIP (Fig. 4), and the higher N:P ratios suggest a stronger P limitation (Sterner and Elser 2002). Light availabilities, may also have been limiting, but did not differ between treatments (Appendix S3: Fig. S3c). At the peak of the phytoplankton spring bloom, chytrid prevalence and rotifer abundance increased (Fig. 5). The phytoplankton spring bloom by *Synedra*, a large diatom in the size range of 75–115 μm (Frenken et al. 2016), was most probably unsuitable as a

food source for the predominant rotifer *Keratella*, which has a body size range of 83–113 μm (Stemberger and Gilbert 1985) and can ingest food particles of 0.5–20 μm (Pourriot 1977). A chytrid epidemic infected up to 40% of the *Synedra* population in both treatments, and the end of this epidemic was advanced in the warm treatment. After the peak of the spring bloom, C:P and N:P ratios were higher in the control treatment and may have imposed elemental constraints on the chytrid development resulting in a delayed phytoplankton bloom termination. This temperature-dependent shift in infection dynamics may explain the lower phytoplankton biomass in the warm treatment during the spring bloom (see also Frenken et al. 2016).

After the phytoplankton spring bloom, DIP concentrations in the water remained low throughout the experiment (Fig. 4b), most probably due to the development of periphyton, benthic algae, and filamentous algae (Appendix S4: Fig. S4). No differences in biomass of periphyton nor those in benthic algae were observed between treatments when focusing on the complete spring-to-summer period (Table 1). In June, periphyton biomass decreased in both treatments, presumably caused by grazing (Appendix S4: Fig. S4). In the control treatment, a second bloom was observed that mainly consisted of the mixotrophic chrysophyte *Dinobryon*, which can occur at low nutrient conditions (van Donk and Ringelberg 1983). In the same period, higher abundance of the predominant cladoceran *Bosmina* was detected in the warm treatment as a result of their advanced timing (Fig. 5c). *Bosmina* is generally considered a filter feeder, but can also consume larger algae by grasping (Bleiwas and Stokes 1985), and may thus possibly have foraged on *Dinobryon*. Advanced grazing pressure in the warm treatment may therefore have prevented the second bloom.

During the heatwave, phytoplankton biomass increased in the control treatment, while it remained low in the warm treatment (Fig. 1). At this point in time, the phytoplankton community consisted mostly of cyanobacteria (*Chroococcus*) and chlorophytes (Appendix S2: Fig. S2). Although higher temperatures generally promote cyanobacteria and chlorophyte growth (Lurling et al. 2013), the heatwave in the warm treatment showed no effect on phytoplankton biomass. Furthermore, no clear changes were observed in

nutrient concentrations (Fig. 4) or in zooplankton abundance (Fig. 5). Higher temperatures may impose physiological constraints on growth, though the maximum temperature of 27°C seemed well in range with growth optima of cyanobacteria as well as chlorophytes (Lurling et al. 2013). It remains unclear what constrained phytoplankton growth during the heatwave in the warm treatment.

Over the course of the experiment, seston C:P and N:P ratios were lower in the warm treatment as compared to the control (Fig. 3, Table 1). Such relatively higher seston P contents may result from higher P availability, as well as from shifts in species composition and size distribution (Friebele et al. 1978, Smith and Kalff 1982, Klausmeier et al. 2004, Hillebrand et al. 2013). As no differences in DIP concentrations were observed between treatments (Fig. 4b), and composition and size distribution of the phytoplankton community remained largely comparable (Fig. 2), these processes seem an unlikely cause for the observed pattern. Phytoplankton biomass was lower in the warm treatment (Fig. 1) and may have led to an increase in per capita P availability and thus lower C:P and N:P ratios. In contrast to our findings, earlier studies have shown increased C:P (under low P; De Senerpont Domis et al. 2014) and N:P (Toseland et al. 2013) ratios with warming that were presumably caused by higher P-use efficiencies and lower demands for P-rich ribosomes, respectively. Such differences in stoichiometric responses of phytoplankton communities to warming may result from the presence of grazers (Biermann et al. 2015), as consumer-driven nutrient recycling may alter phytoplankton carbon:nutrient ratios (Elser and Urabe 1999, Urabe et al. 2002). Furthermore, DIN and CO₂ concentrations increased later on in the experiment, with higher NO₃⁻:NH₄⁺ ratios in the control treatment (Appendix S3: Fig. S3a, b). This suggests enhanced heterotrophic turnover over time, and may possibly indicate an increase in nitrification in the warm treatment (Grundmann et al. 1995). Thus, in our experiment, warming may have enhanced nutrient recycling by heterotrophs and thereby led to reduced seston C:P and N:P ratios.

Chytrids and zooplankton community dynamics

Disease epidemics are expected to be promoted by warming (Harvell et al. 2002, Marcogliese 2008). Indeed, previous analysis from our

experiment showed accelerated development of chytrid prevalence (Frenken et al. 2016), and the chytrid epidemic ended earlier in the warm treatment (Fig. 5a, Table 2). This advanced ending of the chytrid epidemic in the warm treatment may not only be explained by direct temperature effects on the chytrid (Bruning 1991), but also by the observed shifts in host elemental composition indicating a reduced nutritional value for higher trophic levels (Fig. 3, for further details; see Frenken et al. 2016).

We observed changes in zooplankton dynamics in response to warming (Table 1, Fig. 5b–d). This effect is attributed to shifts in phenology, as peaks of all groups advanced in the warm treatment, while no effect on their total abundance was observed (Fig. 5b–d, Table 2). The observed changes in the phenology of rotifers (dominated by *Keratella*), cladocerans (dominated by *Bosmina*), and copepods in response to warming are consistent with earlier reported patterns for ciliates (Aberle et al. 2012), rotifers (Winder and Schindler 2004b), and some studies on daphnids (Adrian et al. 2006, Feuchtmayr et al. 2010). Other studies, however, did not show an effect of warming on the phenology of daphnids (Winder and Schindler 2004b) and copepods (Adrian et al. 2006). The effect of warming on zooplankton phenology thus seems to depend on their community composition. The observed shifts in zooplankton phenology may have resulted from temperature-dependent increases in growth and hatching rates (McFeeters and Frost 2011, Weydmann et al. 2015). Furthermore, warming can positively affect cladoceran and copepod recruitment (Ekvall and Hansson 2012), leading to an advanced occurrence of these groups. Such phenological shifts will have consequences for food-web dynamics, and possibly lead to mismatches between a consumer and its food (Winder and Schindler 2004a). Yet, zooplankton abundance was comparable between both treatments (Table 2), and negative consequences of a possible mismatch were therefore unlikely. In addition, our results demonstrate an advanced top-down control of phytoplankton in response to warming, and thereby suggest a closer coupling between phytoplankton and their grazers. Although the contribution of zooplankton to the explained variance in the phytoplankton dynamics did not differ between treatments (Table 3), subtle differences in group-specific effects could be observed. For

instance, the advanced development of the *Bosmina* population in the warm treatment may have prevented a second phytoplankton bloom. Also, the earlier development of the *Keratella* population may have been facilitated by the chytrid epidemic in the warm treatment, as chytrid zoospores may possibly serve as food source for the rotifers (Schmeller et al. 2014, Frenken et al. 2016).

Variables explaining the variance in phytoplankton chlorophyll-a dynamics

The phytoplankton chlorophyll-*a* dynamics were analyzed with a linear model to assess the contribution of the various variables to the explained variance (Table 3). The applied procedure correlates phytoplankton biomass with all measured variables and determines their relative importance to the overall fit, while correcting for time-dependent dynamics. The linear model captured most of the variance in biomass dynamics of both treatments (i.e., up to 86%). Regardless of temperature treatment, phytoplankton biomass could be explained by the same set of predictors with approximately the same contribution of the individual parameters. Furthermore, we observed a substantial seasonal temperature effect confirming that seasonal warming plays a major role in driving the phytoplankton dynamics (Table 3).

Zooplankton was among the main contributors, indicating strong top-down control. Prevalence of chytrid infection contributed less to the overall chlorophyll-*a* dynamics as they are host specific, and thus only played a role in the dynamics of the *Synedra* spring bloom, not in the dynamics of other phytoplankton groups. Concentrations of inorganic nutrients are closely coupled to phytoplankton biomass build-up. Indeed, inorganic nutrients decreased rapidly during the spring bloom, but subsequently remained low (Si and DIP) or showed an increase only during the end of the experiment (DIN). Consequently, their contribution to the overall chlorophyll-*a* dynamics was relatively low.

CONCLUSIONS

All in all, we show that experimental warming can lead to lowered producer biomass, advanced grazer phenology, and shifts in parasite dynamics during a spring-to-summer period, while the relative contribution of top-down and bottom-up

processes to phytoplankton dynamics remains unaltered. A clear seasonal temperature effect on phytoplankton dynamics was observed, which suggests that seasonal warming plays a major role and may even overrule climate warming effects. Our findings indicate that warming advances top-down control and reduces phytoplankton biomass, thereby demonstrating how bottom-up and top-down related processes can shape future phytoplankton dynamics.

ACKNOWLEDGMENTS

The authors thank Nico Helmsing, Suzanne Wiezer, Erik Reichman, and Niels van de Bospoort for their assistance during the experiment, and Sven Teurlinx and Alena Gsell for their advice on statistical analysis. Furthermore, we would like to thank the anonymous reviewers for their valuable comments on the manuscript. The work of Mandy Velthuis is funded by the Gieskes-Strijbis Foundation; Sarian Kosten was supported by Nederlandse Organisatie voor Wetenschappelijk Onderzoek (NWO) Veni Grant 86312012 and Garabet Kazanjian by the German Leibniz Association (Project Landscapes).

LITERATURE CITED

- Aberle, N., B. Bauer, A. Lewandowska, U. Gaedke, and U. Sommer. 2012. Warming induces shifts in microzooplankton phenology and reduces time-lags between phytoplankton and protozoan production. *Marine Biology* 159:2441–2453.
- Adrian, R., S. Wilhelm, and D. Gerten. 2006. Life-history traits of lake plankton species may govern their phenological response to climate warming. *Global Change Biology* 12:652–661.
- Berger, S. A., S. Diehl, H. Stibor, G. Trommer, and M. Ruhenstroth. 2010. Water temperature and stratification depth independently shift cardinal events during plankton spring succession. *Global Change Biology* 16:1954–1965.
- Biermann, A., A. M. Lewandowska, A. Engel, and U. Riebesell. 2015. Organic matter partitioning and stoichiometry in response to rising water temperature and copepod grazing. *Marine Ecology Progress Series* 522:49–65.
- Bleiwass, A. H., and P. M. Stokes. 1985. Collection of large and small food particles by *Bosmina*. *Limnology and Oceanography* 30:1090–1092.
- Both, C., M. van Asch, R. G. Bijlsma, A. B. van den Burg, and M. E. Visser. 2009. Climate change and unequal phenological changes across four trophic levels: Constraints or adaptations? *Journal of Animal Ecology* 78:73–83.
- Bruning, K. 1991. Effects of temperature and light on the population-dynamics of the *Asterionella-Rhizosphydium* association. *Journal of Plankton Research* 13:707–719.
- Butterwick, C., S. I. Heaney, and J. F. Talling. 2005. Diversity in the influence of temperature on the growth rates of freshwater algae, and its ecological relevance. *Freshwater Biology* 50:291–300.
- De Senerpont Domis, L. N., D. B. Van de Waal, N. R. Helmsing, E. van Donk, and W. M. Mooij. 2014. Community stoichiometry in a changing world: combined effects of warming and eutrophication on phytoplankton dynamics. *Ecology* 95:1485–1495.
- De Senerpont Domis, L. N., et al. 2013. Plankton dynamics under different climatic conditions in space and time. *Freshwater Biology* 58:463–482.
- Dickson, A. G., and F. J. Millero. 1987. A comparison of the equilibrium constants for the dissociation of carbonic acid in seawater media. *Deep Sea Research. Part A, Oceanographic Research Papers* 34:1733–1743.
- Donnelly, A., A. Caffarra, and B. F. O'Neill. 2011. A review of climate-driven mismatches between interdependent phenophases in terrestrial and aquatic ecosystems. *International Journal of Biometeorology* 55:805–817.
- Ekvall, M. K., and L. A. Hansson. 2012. Differences in Recruitment and life-history strategy alter zooplankton spring dynamics under climate-change conditions. *PLoS ONE* 7:e44614.
- Elser, J. J., and J. Urabe. 1999. The stoichiometry of consumer-driven nutrient recycling: theory, observations, and consequences. *Ecology* 80:735–751.
- Feuchtmayr, H., B. Moss, I. Harvey, R. Moran, K. Hatton, L. Connor, and D. Atkinson. 2010. Differential effects of warming and nutrient loading on the timing and size of the spring zooplankton peak: an experimental approach with hypertrophic freshwater mesocosms. *Journal of Plankton Research* 32:1715–1725.
- Frenken, T., M. Velthuis, L. N. De Senerpont Domis, S. Stephan, R. Aben, S. Kosten, E. van Donk, and D. B. Van de Waal. 2016. Warming accelerates termination of a phytoplankton spring bloom by fungal parasites. *Global Change Biology* 22:299–309.
- Friebele, E. S., D. L. Correll, and M. A. Faust. 1978. Relationship between phytoplankton cell size and the rate of orthophosphate uptake: in situ observations of an estuarine population. *Marine Biology* 45:39–52.
- Grömping, U. 2006. Relative importance for linear regression in R: the package relaimpo. *Journal of Statistical Software* 17:1–27.

- Grundmann, G. L., P. Renault, L. Rosso, and R. Bardin. 1995. Differential effects of soil water content and temperature on nitrification and aeration. *Soil Science Society of America Journal* 59: 1342–1349.
- Gsell, A. S., L. N. De Senerpont Domis, S. M. H. Naus-Wiezer, N. R. Helmsing, E. van Donk, and B. W. Ibelings. 2013. Spatiotemporal variation in the distribution of chytrid parasites in diatom host populations. *Freshwater Biology* 58:523–537.
- Gudas, C., D. Bastviken, K. Steger, K. Premke, S. Sobek, and L. J. Tranvik. 2010. Temperature-controlled organic carbon mineralization in lake sediments. *Nature* 466:478–481.
- Hansson, L.-A., A. Nicolle, W. Granéli, P. Hallgren, E. Kritzberg, A. Persson, J. Björk, P. A. Nilsson, and C. Brönmark. 2013. Food-chain length alters community responses to global change in aquatic systems. *Nature Climate Change* 3:228–233.
- Harrison, R. M. 2007. *Principles of environmental chemistry*. RSC Publishing, Cambridge, UK.
- Harvell, C. D., C. E. Mitchell, J. R. Ward, S. Altizer, A. P. Dobson, R. S. Ostfeld, and M. D. Samuel. 2002. Climate warming and disease risks for terrestrial and marine biota. *Science* 296:2158–2162.
- Hillebrand, H., G. Steinert, M. Boersma, A. Malzahn, C. L. Meunier, C. Plum, and R. Ptacnik. 2013. Goldman revisited: Faster-growing phytoplankton has lower N: P and lower stoichiometric flexibility. *Limnology and Oceanography* 58:2076–2088.
- Hyndman, R. J. 2015. {forecast}: forecasting functions for time series and linear models. R package version 6.2. <http://github.com/robjhyndman/forecast>
- Ibelings, B. W., A. de Bruin, M. Kagami, M. Rijkeboer, M. Brehm, and E. van Donk. 2004. Host parasite interactions between freshwater phytoplankton and chytrid fungi (*Chytridiomycota*). *Journal of Phycology* 40:437–453.
- Ibelings, B. W., A. S. Gsell, W. M. Mooij, E. van Donk, S. van den Wyngaert, and L. N. De Senerpont Domis. 2011. Chytrid infections and diatom spring blooms: paradoxical effects of climate warming on fungal epidemics in lakes. *Freshwater Biology* 56:754–766.
- IPCC. 2014. *Climate change 2014: synthesis report*. In *Change Core Writing Team, R. K. Pachauri, and L. A. Meyer, editors. Contribution of Working Groups I, II and III to the Fifth Assessment Report of the Intergovernmental Panel on Climate*. IPCC, Geneva, Switzerland.
- Jensen, T. C., and A. M. Verschoor. 2004. Effects of food quality on life history of the rotifer *Brachionus calyciflorus* Pallas. *Freshwater Biology* 49:1138–1151.
- Jeppesen, E., et al. 2009. Climate change effects on runoff, catchment phosphorus loading and lake ecological state, and potential adaptations. *Journal of Environmental Quality* 38:1930–1941.
- Kauler, P., and H. E. Enesco. 2011. The effect of temperature on life history parameters and cost of reproduction in the rotifer *Brachionus calyciflorus*. *Journal of Freshwater Ecology* 26:399–408.
- Klausmeier, C. A., E. Litchman, T. Daufresne, and S. A. Levin. 2004. Optimal nitrogen-to-phosphorus stoichiometry of phytoplankton. *Nature* 429:171–174.
- Kosten, S., et al. 2012. Warmer climates boost cyanobacterial dominance in shallow lakes. *Global Change Biology* 18:118–126.
- Kratina, P., H. S. Greig, P. L. Thompson, T. S. A. Carvalho-Pereira, and J. B. Shurin. 2012. Warming modifies trophic cascades and eutrophication in experimental freshwater communities. *Ecology* 93:1421–1430.
- Lewandowska, A. M., D. G. Boyce, M. Hofmann, B. Matthiessen, U. Sommer, and B. Worm. 2014. Effects of sea surface warming on marine plankton. *Ecology Letters* 17:614–623.
- Lorenzen, C. J. 1967. Determination of chlorophyll and phaeo-pigments: spectrophotometric equations. *Limnology and Oceanography* 12:343–346.
- Lurling, M., F. Eshetu, E. J. Faassen, S. Kosten, and V. L. M. Huszar. 2013. Comparison of cyanobacterial and green algal growth rates at different temperatures. *Freshwater Biology* 58:552–559.
- Marcollese, D. J. 2008. The impact of climate change on the parasites and infectious diseases of aquatic animals. *Revue Scientifique et Technique (International Office of Epizootics)* 27:467–484.
- Mazaris, A. D., A. S. Kallimanis, S. P. Sgardelis, and J. D. Pantis. 2008. Do long-term changes in sea surface temperature at the breeding areas affect the breeding dates and reproduction performance of Mediterranean loggerhead turtles? Implications for climate change. *Journal of Experimental Marine Biology and Ecology* 367:219–226.
- McFeeters, B. J., and P. C. Frost. 2011. Temperature and the effects of elemental food quality on *Daphnia*. *Freshwater Biology* 56:1447–1455.
- O'Connor, M. I., M. F. Piehler, D. M. Leech, A. Anton, and J. F. Bruno. 2009. Warming and resource availability shift food web structure and metabolism. *Plos Biology* 7:e1000178.
- O'Neil, J. M., T. W. Davis, M. A. Burford, and C. J. Gobler. 2012. The rise of harmful cyanobacteria blooms: the potential roles of eutrophication and climate change. *Harmful Algae* 14:313–334.
- Paerl, H. W., and J. Huisman. 2008. Blooms like it hot. *Science* 320:57–58.

- Pinheiro, J., D. Bates, S. DebRoy, D. Sarkar, and R-Core-Team. 2015. {nlme}: linear and nonlinear mixed effects models. R package version 3.1-121. <http://CRAN.R-project.org/package=nlme>
- Polovina, J. J., E. A. Howell, and M. Abecassis. 2008. Ocean's least productive waters are expanding. *Geophysical Research Letters* 35:L03618.
- Pontin, R. M. 1978. A key to the freshwater planktonic and semi-planktonic Rotifera of the British Isles; Scientific Publication No. 38. Freshwater Biological Association, Ambleside, England, UK.
- Pourriot, R. 1977. Food and feeding habits of Rotifera. *Archiv für Hydrobiologie Beiheft Ergebnisse der Limnologie* 8:243–260.
- R Core Team. 2015. R: a language and environment for statistical computing. R Foundation for Statistical Computing, Vienna, Austria. <https://www.R-project.org/>
- Rasconi, S., M. Jobard, L. Jouve, and T. Sime-Ngando. 2009. Use of calcofluor white for detection, identification, and quantification of phytoplanktonic fungal parasites. *Applied and Environmental Microbiology* 75:2545–2553.
- Rhee, G. Y., and I. J. Gotham. 1981. The effect of environmental factors on phytoplankton growth: temperature and the interactions of temperature with nutrient limitation. *Limnology and Oceanography* 26:635–648.
- Roijackers, R. M. M. 1981. Chrysophyceae from freshwater localities near Nijmegen, The Netherlands. *Hydrobiologia* 76:179–189.
- Rolinski, S., H. Horn, T. Petzoldt, and L. Paul. 2007. Identifying cardinal dates in phytoplankton time series to enable the analysis of long-term trends. *Oecologia* 153:997–1008.
- Schmeller, D. S., et al. 2014. Microscopic aquatic predators strongly affect infection dynamics of a globally emerged pathogen. *Current Biology* 24:176–180.
- Shurin, J. B., J. L. Clasen, H. S. Greig, P. Kratina, and P. L. Thompson. 2012. Warming shifts top-down and bottom-up control of pond food web structure and function. *Philosophical Transactions of the Royal Society B* 367:3008–3017.
- Smith, R. E. H., and J. Kalff. 1982. Size-dependent phosphorus uptake kinetics and cell quota in phytoplankton. *Journal of Phycology* 18:275–284.
- Sommer, U., N. Aberle, K. Lengfellner, and A. Lewandowska. 2012. The Baltic Sea spring phytoplankton bloom in a changing climate: an experimental approach. *Marine Biology* 159:2479–2490.
- Sommer, U., Z. M. Gliwicz, W. Lampert, and A. Duncan. 1986. The PEG-model of seasonal succession of planktonic events in fresh waters. *Archiv für Hydrobiologie* 106:433–471.
- Stefanescu, C., J. Peñuelas, and I. Filella. 2003. Effects of climatic change on the phenology of butterflies in the northwest Mediterranean Basin. *Global Change Biology* 9:1494–1506.
- Stemberger, R. S., and J. J. Gilbert. 1985. Body size, food concentration, and population growth in planktonic Rotifers. *Ecology* 66:1151–1159.
- Sterner, R. W., and J. J. Elser. 2002. Ecological stoichiometry: the biology of elements from molecules to the biosphere. Princeton University Press, Princeton, New Jersey, USA.
- Strecker, A. L., T. P. Cobb, and R. D. Vinebrooke. 2004. Effects of experimental greenhouse warming on phytoplankton and zooplankton communities in fishless alpine ponds. *Limnology and Oceanography* 49:1182–1190.
- Toseland, A., et al. 2013. The impact of temperature on marine phytoplankton resource allocation and metabolism. *Nature Climate Change* 3:979–984.
- Urabe, J., J. J. Elser, M. Kyle, T. Yoshida, T. Sekino, and Z. Kawabata. 2002. Herbivorous animals can mitigate unfavourable ratios of energy and material supplies by enhancing nutrient recycling. *Ecology Letters* 5:177–185.
- Urabe, J., J. Togari, and J. J. Elser. 2003. Stoichiometric impacts of increased carbon dioxide on a planktonic herbivore. *Global Change Biology* 9:818–825.
- van Donk, E., and S. S. Kilham. 1990. Temperature effects on silicon- and phosphorus-limited growth and competitive interactions among three diatoms. *Journal of Phycology* 26:40–50.
- van Donk, E., and J. Ringelberg. 1983. The effect of fungal parasitism on the succession of diatoms in lake Maarsseveen-I (The Netherlands). *Freshwater Biology* 13:241–251.
- Venables, W. N., and B. D. Ripley. 2002. Modern applied statistics with S. Fourth edition. Springer, New York, New York, USA.
- Verschoor, A. M., J. Takken, B. Massieux, and J. Vijverberg. 2003. The Limnotrons: a facility for experimental community and food web research. *Hydrobiologia* 491:357–377.
- Weydmann, A., A. Zwolicki, K. Muś, and S. Kwaśniewski. 2015. The effect of temperature on egg development rate and hatching success in *Calanus glacialis* and *C. finmarchicus*. *Polar Research* 34:23947.
- Winder, M., and D. E. Schindler. 2004a. Climate change uncouples trophic interactions in an aquatic ecosystem. *Ecology* 85:2100–2106.
- Winder, M., and D. E. Schindler. 2004b. Climatic effects on the phenology of lake processes. *Global Change Biology* 10:1844–1856.

- Witty, L. M. 2004. Practical guide to identifying freshwater crustacean zooplankton. Cooperative Freshwater Ecology Unit, Sudbury, Ontario, Canada.
- Yvon-Durocher, G., J. M. Montoya, M. Trimmer, and G. Woodward. 2011. Warming alters the size spectrum and shifts the distribution of biomass in freshwater ecosystems. *Global Change Biology* 17:1681–1694.
- Zeileis, A., and G. Grothendieck. 2005. zoo: S3 infrastructure for regular and irregular time series. *Journal of Statistical Software* 14:1–27.

SUPPORTING INFORMATION

Additional Supporting Information may be found online at: <http://onlinelibrary.wiley.com/doi/10.1002/ecs2.1651/full>